Fast and Slow Dynamics of Water-Soluble Dendrimers Consisting of Amido-Amine Repeating Units by Neutron Spin−Echo

Katsuya Funayama,[†] Toyoko Imae,*[,†,‡] Hideki Seto,[§] Keigo Aoi,[||] Kaname Tsutsumiuchi,[||] Masahiko Okada,[||] Michihiro Nagao,[⊥] and Michihiro Furusaka[#]

Graduate School of Science and Research Center for Materials Science, Nagoya University, Chikusa, Nagoya 464-8602, Japan, Faculty of Integrated Arts and Sciences, Hiroshima University, Higashihiroshima 739-8521, Japan, Graduate School of Bioagricultural Sciences, Nagoya University, Chikusa, Nagoya 464-8601, Japan, Institute for Solid State Physics, The University of Tokyo, Tokai 319-1106, Japan, and Institute of Materials Structure Science, High Energy Accelerator Research Organization, Tsukuba 305-0801, Japan

Received: September 13, 2002; In Final Form: November 25, 2002

Neutron spin−echo (NSE) experiments were performed at room temperature on D_2O solutions of fifth generation poly(amido amine) (PAMAM) dendrimers with different types of end groups. Intermediate correlation functions $I(Q,t)/I(Q,0)$ at different scattering vectors Q as a function of time t show different dynamics for dendrimer concentrations of 1.0 and 10 wt %, while the dynamics was independent of the chemical species of the end groups, hydroxyl or glucopeptide. The NSE results for a 10 wt % solution followed a single-exponential decay. With increasing Q, the evaluated effective diffusion coefficients D_{eff} decreased and converged to the translational diffusion coefficient D_0, which was obtained from dynamic light scattering. It is assumed that the Q-dependence of D_{eff} is caused by the dendrimer-dendrimer interaction, which is observed as the inter-dendrimer structure factor on small-angle neutron scattering. On the other hand, NSE results for a 1.0 wt % solution were well-fitted to a double-exponential function with two decay rates (fast and slow modes). It was observed that the diffusion coefficient of the slow mode corresponds to D_0. The fast mode originates from the motion of amido-amine segments in the dendrimer, which is a common internal unit for the two dendrimers.

Introduction

Our knowledge on molecular dynamics has been increased mainly due to the notable progress of scattering techniques. Neutron spin−echo (NSE), informing inelastic dynamics, is viewed as an extension of small-angle neutron scattering (SANS). The NSE method proposed by Mezei[1] provides an extremely high resolution in the analysis of small energy changes on scattering, as a phase shift in the Larmor precession of neutron spin within a magnetic field. Therefore, this technique is suitable for the investigation of local molecular dynamics. Kanaya et al.[2] investigated polyelectrolyte solutions in water without added salts. From the scattering vector-dependent effective diffusion coefficient, it was found that the transition from dilute to semidilute region occurs at a critical molecular weight. Farago et al.[3] investigated spherical micelles of polystyrene-polyisoprene diblock copolymers in *n*-decane by NSE and observed the thermal density fluctuation of the polyisoprene corona. Ewen and Richter[4] and Richter[5] examined polymers in dense systems and discussed the internal segment diffusion of long chains and the existence of entanglements in melt. Molecular motions of poly(1,4-butadiene) and polyisobutylene were reported by Arbe et al.[6] and Richter et al.,[7] respectively. Monkenbusch et al.[8] studied platelet-like aggregates of polyethylene−polyethylenebutylene copolymers in decane and found the fluctuation dynamics on the surface of a polymeric brush. Very recently, Matsuoka et al.[9] examined the dynamics of micelles of an amphiphilic diblock copolymer in aqueous solutions. They obtained fast and slow modes on the time-correlation function for the polymer micelles. Monkenbusch et al.[10] and Arbe et al.[11] discussed chain dynamics in melt and in dilute solutions of flexible polymers and compared the dynamics of two flexible polymers which exhibit the same static rigidity.

Dendrimers[12,13] are a novel class of macromolecules, and their size and shape are comparable to micelles which are spherical nanoparticles self-assembled in solutions. One expects, therefore, that dendrimers function as monomolecular micelles and that additional novel functions will originate because of the dendrimers' regularly branching and spongelike structure. The functions of dendrimers are affected by the dynamics of the dendrimer itself. Then dendrimers are a fascinating object for NSE experiments. Although several investigations on dendrimers were performed by small-angle neutron scattering,[14−23] only one application of NSE has ever been reported.[24]

In the present paper, we investigate solutions of fifth generation (G5) poly(amide amine) (PAMAM) dendrimers with hydroxyl end groups (OH−PAMAM dendrimer) and galactose-having glycopeptide end groups (sugar ball) by SANS and NSE. The end groups of both dendrimers are hydrophilic but differ regarding their size and spatial conformations. The G5 OH−PAMAM dendrimer (Figure 1a) has a spongelike spherical

* To whom correspondence should be addressed. Address: Research Center for Materials Science, Nagoya University, Chikusa, Nagoya 464-8602, Japan. E-mail: imae@nano.chem.nagoya-u.ac.jp.
[†] Graduate School of Science.
[‡] Research Center for Materials Science.
[§] Faculty of Integrated Arts and Sciences.
[||] Graduate School of Bioagricultural Sciences.
[⊥] Institute for Solid State Physics.
[#] Institute of Materials Structure Science.

10.1021/jp0269874 CCC: $25.00
Published on Web 01/11/2003

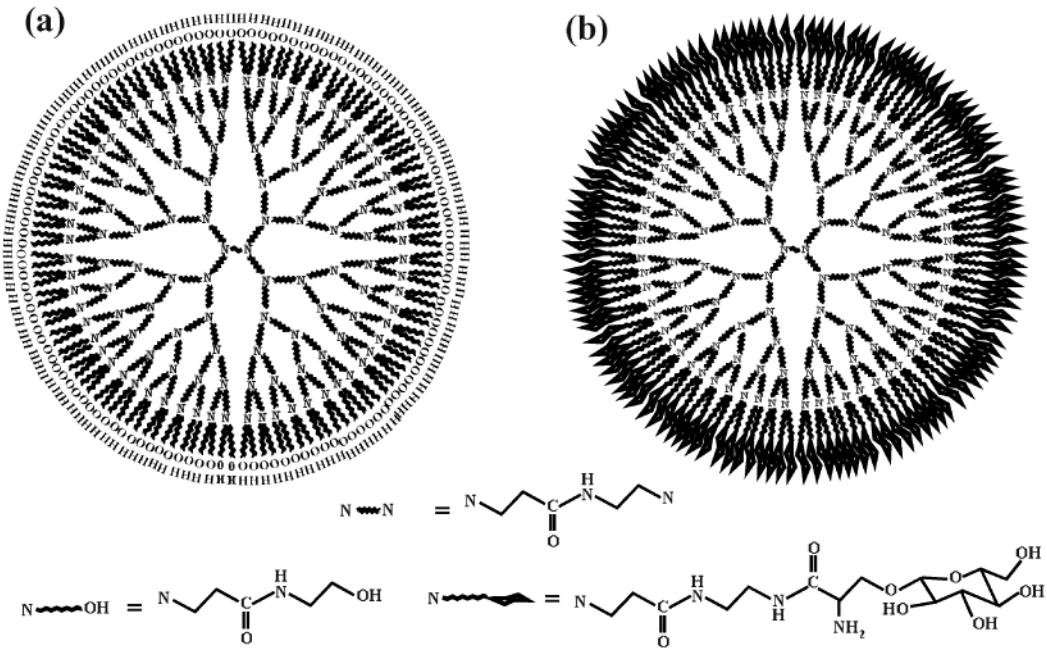

Figure 1. Chemical structures of G5 dendrimers. (a) OH−PAMAM dendrimer and (b) sugar ball.

structure and its segment density is the largest at the fourth layer, while the penetrated solvent is the most dominant at the fifth layer.[18,19] On the other hand, the G5 sugar ball (Figure 1b) has a dense shell and behaves like a rigid sphere.[25,26] The influence of the branching structure and dendrimer concentration on molecular dynamics in solutions was already discussed.[24]

By means of quasielastic neutron scattering, Stark et al.[27] investigated the dynamics of carbosilane dendrimer with perfluorohexyl ($-C_6F_{13}$) end groups. For low generations (G1−G3), they observed the segmental diffusion in the dendrimer core and the rotational diffusion of the end groups. In a theoretical approach, Chen and Cai[28] calculated diffusion coefficients of starburst dendrimers and compared with those for PAMAM dendrimers[28] and carbosilane dendrimers.[27] The relaxation times theoretically determined are faster than those of carbosilane and PAMAM dendrimers. Very recently Ganazzoli et al.[29] derived theoretically the dynamical properties of dendrimers in dilute solutions. Their important outcome is the qualitative similarity between the results obtained under good solvent conditions and by stiff models. In this paper, we have tried to clarify the relationship between the dendrimer end groups and the molecular dynamics in a high-generation dendrimer.

Experimental Section

Dendrimers. The G5 OH−PAMAM dendrimer was synthesized by the reaction of 2-aminoethanol with 4.5th-generation PAMAM dendrimer [ethylenediamine core] having methyl ester end groups, as reported before.[12,18] The G5 sugar ball was prepared by radial-growth polymerization of sugar-substituted α-amino acid *N*-carboxyanhydride on G5 PAMAM dendrimer with amino end groups.[25,26] The number of terminal hydroxyl groups of G5 sugar balls was determined to be 113 by ^{1}H NMR and then the calculated molecular weight is 54900. From dynamic light scattering (DLS) measurements at a scattering angle of 90° for 1.0 wt % dendrimer solutions in H_2O, the translational diffusion coefficients D_0 for G5 OH−PAMAM dendrimers and sugar balls were obtained to be 6.5×10^{-11} and 4.4×10^{-11} m^2/s, respectively. Then the hydrodynamic radii R_h were 39 and 54 Å, respectively.

D_2O (99.75%) was purchased from Wako Pure Chemical Industries, Ltd, Osaka. Dendrimer solutions in D_2O were prepared at two concentrations, 1.0 and 10 wt %.

Measurements. SANS measurements were performed using the cold neutron small-angle scattering facility WINK in KEK (Tsukuba, Japan) and the SANS−U diffractometer [detector-to-sample distance: 1, 4, and 8 m] of the JRR-3M reactor in JAERI (Tokai, Japan). The neutron radiation wavelength of the WINK and SANS−U instruments were $\lambda = 1-16$ and 4−10 Å, respectively. The distribution $\Delta\lambda/\lambda$ for the SANS-U instrument was 10−30%. Rectangular quartz cells of (width) 22 × (height) 40 × (depth) 2 mm^3 for WINK and (width) 10 × (height) 40 × (depth) 2 mm^3 for SANS-U were used for the measurements at room temperature (∼25 °C). The radial-averaged data were calibrated for the background scattering, the intensity from the cell and the solvent, the transmission of the solution, and the thickness of the cell.[30−32] Moreover, the data from the SANS-U were obtained at an absolute scale by calibration with the standard sample, luporen.

NSE measurements[33,34] were carried out at room temperature (∼25 °C), using a NSE spectrometer on the cold neutron beam port C2-2 in the JRR-3M reactor, Tokai. Neutron beams of wavelengths $\lambda = 5.9$ and 7.1 Å with distributions $\Delta\lambda/\lambda = 15$ and 18%, respectively, were used. The scattering vector Q range was 0.02 Å^{-1}−0.1 Å^{-1}, and the time range covered was $0.15 \le t \le 15$ ns. Solutions were contained in a rectangular quartz cell of (width) 40 × (height) 40 × (depth) 2 mm^3. The intermediate correlation functions $I(Q,t)$ at a time t were normalized by the elastic scattering intensity $I(Q,0)$ of a standard sample, Grafoil, at each scattering angle.

Results

Figure 2 shows double-logarithmic plots of the SANS intensity $I(Q)$ versus the scattering vector Q for the solutions of G5 OH−PAMAM dendrimers and sugar balls at 1.0 and 10 wt %. As it can be observed for both dendrimers, a different Q dependence of $I(Q)$ for different dendrimer concentrations is obtained within the Q range examined here. The SANS intensity for dendrimer solutions can be described by[31]

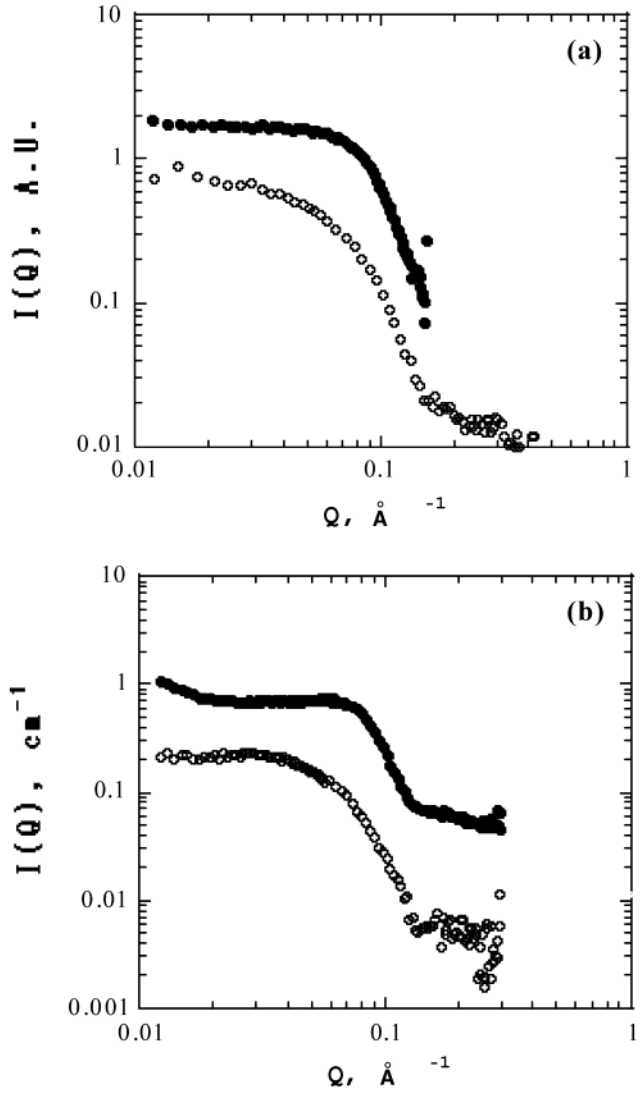

Figure 2. SANS intensity $I(Q)$, as a function of the scattering vector Q, for D_2O solutions of G5 dendrimers. (a) OH−PAMAM dendrimer and (b) sugar ball. Concentration (wt %): ●, 10; ○, 1.0.

$$I(Q) = n_p P(Q) S(Q) \quad (1)$$

where n_p is the number density of dendrimer molecules. *P(Q)* is the intra-dendrimer form factor, which depends on the dendrimer geometry. *S(Q)* is the inter-dendrimer structure factor, and it is related to the inter-dendrimer interactions. For dilute solutions, such as 1.0 wt %, the inter-dendrimer interaction can be approximated to unity.[14,15,18,30] On the other hand, the scattering profiles for 10 wt % solutions include the effect of the inter-dendrimer interaction. It appears as an increase of the scattering intensity at $Q = 0.02 \sim 0.1$ Å^{-1} or a broad peak at $Q = 0.06-0.08$ Å^{-1} in comparison with the scattering curves of 1.0 wt % solutions. The structural analysis of dendrimers based on SANS results of low concentration systems was carried out elsewhere.[18,35] NSE experiments were carried out at a Q range, where the Q dependence of $I(Q)$ was remarkable.

The intermediate correlation function *I(Q,t)* of an investigated system, depending on the wave vector Q and Fourier time t, is observed in the NSE measurement. In the quasielastic scattering, $I(Q,t)$ is simply proportional to the spin−echo signal amplitude at the spin−echo condition. Normalized intermediate scattering functions $I(Q,t)/I(Q,0)$ as a function of time t, observed at different scattering vectors, for 10 and 1.0 wt % solutions of OH−PAMAM dendrimers, are plotted in Figure 3. When only one diffusion mode contributes to the dendrimer dynamics, the scattering function is described by a single-decaying exponential function, which is expressed as

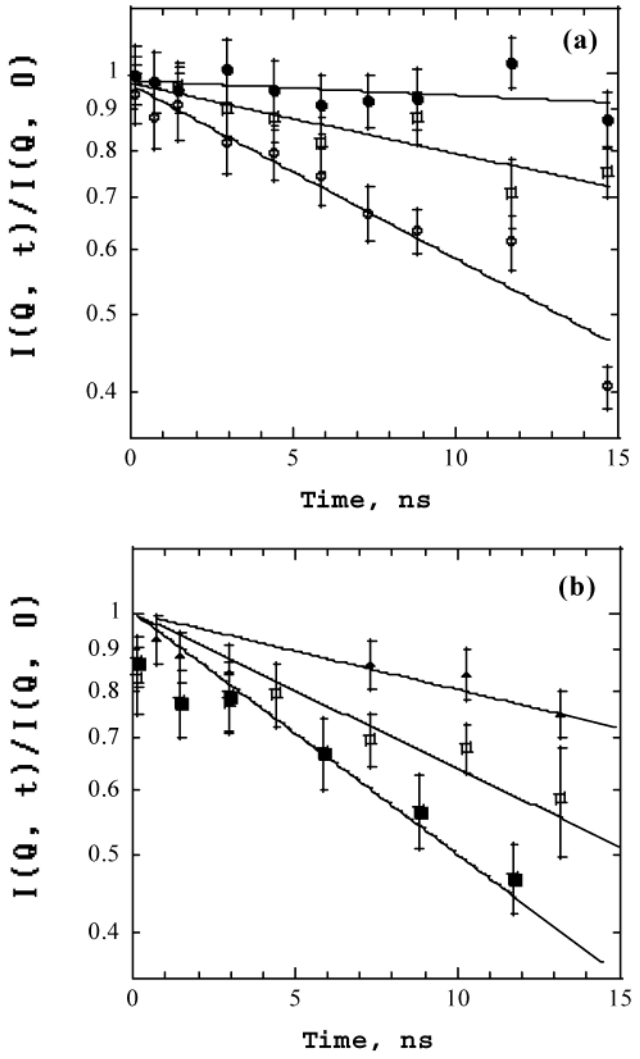

Figure 3. Normalized intermediate scattering function $I(Q,t)/I(Q,0)$, as a function of time t, for D_2O solutions of G5 OH−PAMAM dendrimers. Concentration (wt %): (a) 10 and (b) 1.0. Q (Å^{-1}): ●, 0.02; ▲, 0.04; □, 0.06; ■, 0.08; ○, 0.1. Solid lines are theoretical ones calculated with a single-decaying exponential function (eq 2).

$$\frac{I(Q,t)}{I(Q,0)} = \exp(-\Gamma(Q)t) \quad (2)$$

where $\Gamma(Q)$ is the decay rate.[2] As seen in Figure 3a, the experimental data for a 10 wt % solution can be well described by the eq 2. It is, however, apparent that the data at 1.0 wt % do not obey the same function, as seen in Figure 3b. Figure 4 shows $I(Q,t)/I(Q,0)$ as a function of t for 10 and 1.0 wt % solutions of sugar balls. Again it is observed that eq 2 is adequate to interpret the NSE results for a 10 wt % solution of sugar balls (Figure 4a) but not for a 1.0 wt % solution (Figure 4 (b)).

The decay rate $\Gamma(Q)$, evaluated from eq 2, for 10 wt % solutions, is related to the effective diffusion coefficient D_{eff} according to the expression[36]

$$\Gamma(Q) = D_{eff} Q^2 \quad (3)$$

Figure 5 shows the effective diffusion coefficient D_{eff} as a function of Q for 10 wt % solutions of OH−PAMAM

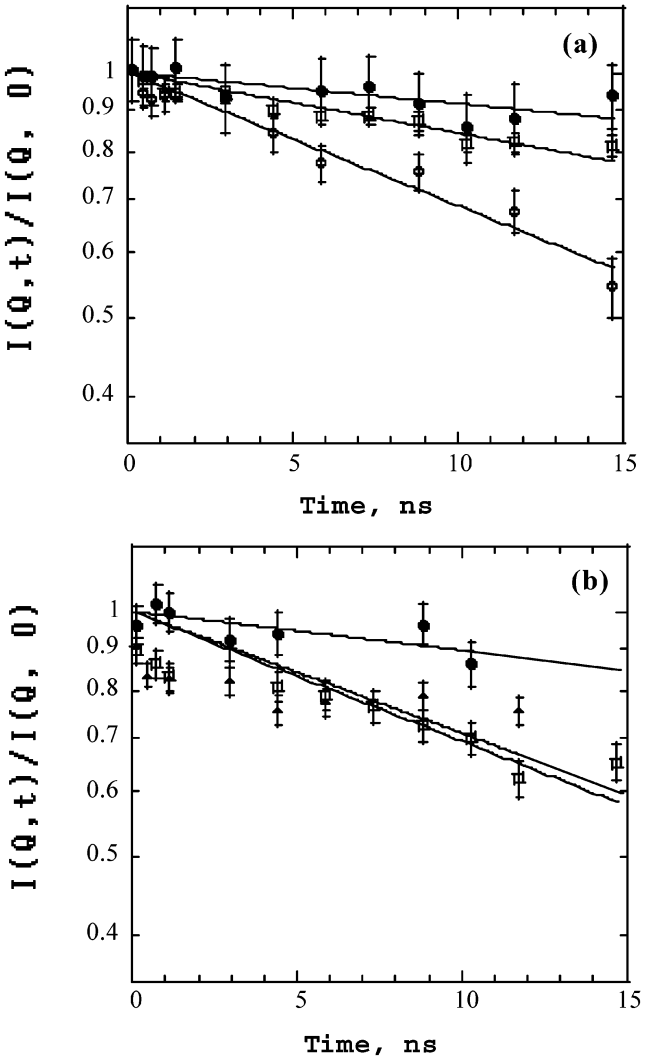

Figure 4. Normalized intermediate scattering function $I(Q,t)/I(Q,0)$, as a function of time t, for D_2O solutions of G5 sugar balls. Concentration (wt %): (a) 10 and (b) 1.0. Legends of symbols and solid lines are the same as in Figure 3.

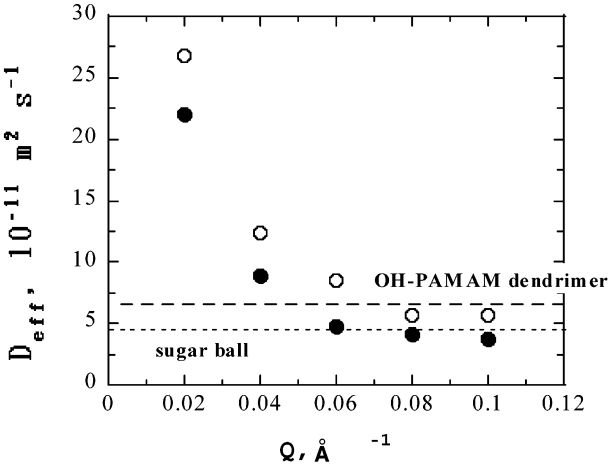

Figure 5. Effective diffusion coefficient D_{eff} as a function of Q, for G5 dendrimers in 10 wt % solutions. ○, OH−PAMAM dendrimer; ●, sugar ball. Broken and dotted horizontal lines represent the translational diffusion coefficient D_0, obtained by DLS, for OH−PAMAM dendrimer and sugar ball, respectively.

dendrimers and sugar balls. For both dendrimer solutions, the D_{eff} values decrease with increasing Q, approaching a constant value for high Q values. The constant values obtained at high Qs are similar to the translational diffusion coefficients D_0 of the dendrimers obtained by DLS, as it was mentioned in the Experimental Section.

Discussion

From NSE results one can say that the dynamics of PAMAM dendrimers in solutions depends on the concentration but not on the type of the end groups. The dynamics, therefore, results from the common architecture of OH−PAMAM dendrimers and sugar balls, that is, the regularly branching amido-amine repeating unit. Now, it must be clarified what kind of diffusion behaviors exist, at each concentration, in the dendrimer solutions. The mode, where the droplet fluctuates and deforms from the spherical shape, has been already reported for microemulsion systems.[37,38] For such case, there must be a clear peak, the position of which corresponds to the molecular size deduced from dynamic light scattering. However, this mode is not observed in the present systems of OH−PAMAM dendrimers and sugar balls, since there are no peaks in the Q region around 0.08 and 0.06 $Å^{-1}$, respectively, in Figure 5.

The D_{eff} values obtained can be compared with those obtained from SANS. According to the discussion mentioned in the previous section, SANS intensities for the 1.0 and 10 wt % solutions, respectively, can be represented by

$$I_{1wt\%}(Q) = n_{p,1wt\%} P(Q) \tag{4}$$

$$I_{10wt\%}(Q) = 10 n_{p,1wt\%} P(Q) S(Q) \tag{5}$$

Then, the inter-dendrimer structure factor $S(Q)$ for a 10 wt % solution can be evaluated by dividing the SANS intensity $I_{10wt\%}(Q)$ by $I_{1wt\%}(Q)$. In Figure 6 the obtained inter-dendrimer structure factor $S(Q)$ is compared with the reciprocal of the effective diffusion coefficient D_{eff} calculated for 10 wt % dendrimer solutions. The depression of D_{eff}^{-1} observed in the low Q region for both dendrimers is similar to that found for the evaluated $S(Q)$. This suggests that the behaviors of both D_{eff}^{-1} and $S(Q)$ are related to the dendrimer−dendrimer interactions.

As it was stated above, NSE data for 1.0 wt % solutions of dendrimer do not obey a single-exponential function. Therefore, those data were analyzed using a function with two exponential relaxation modes[9,39] with

$$\frac{I(Q,t)}{I(Q,0)} = f_S \exp(\Gamma_S t) + f_F \exp(\Gamma_F t) \tag{6}$$

$$f_S + f_F = 1 \tag{7}$$

and

$$\Gamma_S = D_S Q^2, \quad \Gamma_F = D_F Q^2 \tag{8}$$

where f is a fraction of the contribution of each decay mode, and subscripts S and F denote slow and fast modes, respectively.

The experimental NSE data for 1.0 wt % solutions were analyzed using eqs 6−8 introducing the value of D_0 obtained from DLS as D_s. The optimum parameters obtained from the fittings are listed in Table 1 and the calculated curves are shown in Figure 7. The contribution f_F of the fast mode is always small as compared with that of the slow mode, as it is seen in Table 1. The f_F value increases with increasing the Q value. This can be taken as an indication that the fast mode results from the microscopic motion of dendrimers. The fast mode was not

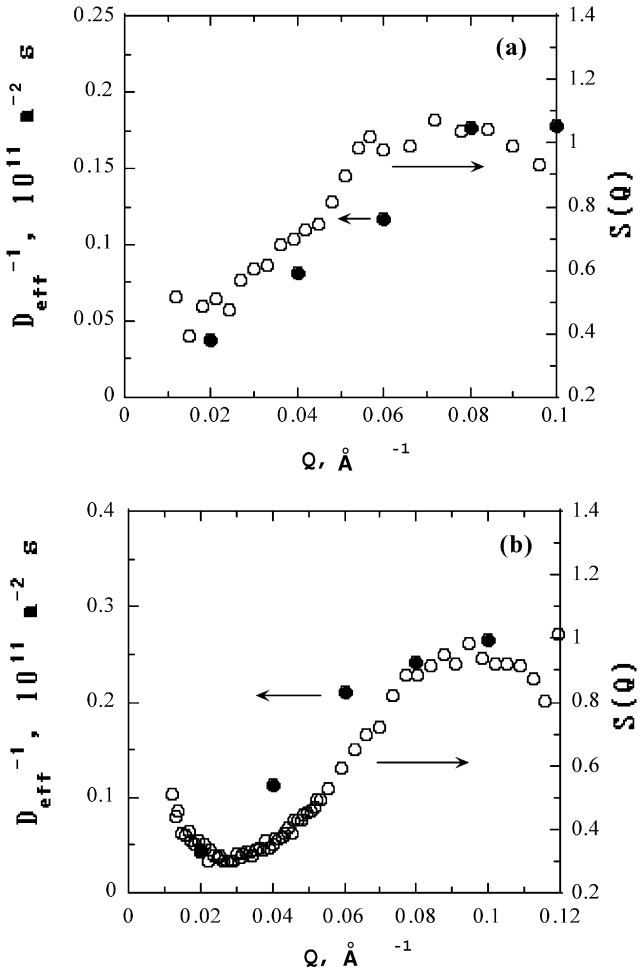

Figure 6. Reciprocal of the effective diffusion coefficient ●, D_{eff} and the inter-dendrimer structure factor ○, $S(Q)$ as a function of Q, for 10 wt % solutions of G5 dendrimers. (a) OH−PAMAM dendrimer and (b) sugar ball.

TABLE 1: Optimum Parameters Obtained for a Double-Exponential Equation (Equations 6−8) for 1.0 wt % Solutions of Dendrimers

dendrimer	Q, Å^{-1}	f_S	f_F	Γ_f, ns^{-1}	D_f, 10^{-8} m^2 s^{-1}
OH−PAMAM dendrimer	0.04	0.90	0.10	3	1.9
	0.06	0.84	0.16	8	2.2
	0.08	0.83	0.17	13	2.0
sugar ball	0.02	0.96	0.04	0.4	1.1
	0.04	0.82	0.18	5	3.1
	0.06	0.87	0.13	12	3.2

observed for the 10 wt % solutions of dendrimers. Dendrimers have fast and slow intrinsic modes, which are attributed to the segment motion in the dendrimer and the translational diffusion motion of dendrimer, respectively. When the dendrimer concentration increases, the additional dendrimer−dendrimer interaction occurs and contributes to the slow mode. Then, the fast mode was embedded into the slow mode with the additional contribution of the dendrimer−dendrimer interaction because of the smaller contribution of the fast mode. It should be noted that this contribution is not due to the solvent, and therefore, it is different from the analysis proposed by Monkenbusch et al.[10]

Quasielastic neutron scattering measurements by Stark et al.[27] demonstrated the properties of the microscopic dynamics in low-generation (G1-G3) carbosilane dendrimers. Increasing the generation number slows down the segmental diffusion and extends the lifetime of local dynamical processes. On the other hand, the rotational diffusion of the end groups is not strongly affected by the generation number. However, higher generation (G5) PAMAM dendrimers observed by NSE in the present work display microscopic dynamics with faster relaxation modes than those reported for the carbosilane dendrimer. It seems, therefore, that the dendrimers used in the present work have larger free void in the interior layers as compared with carbosilane dendrimers.

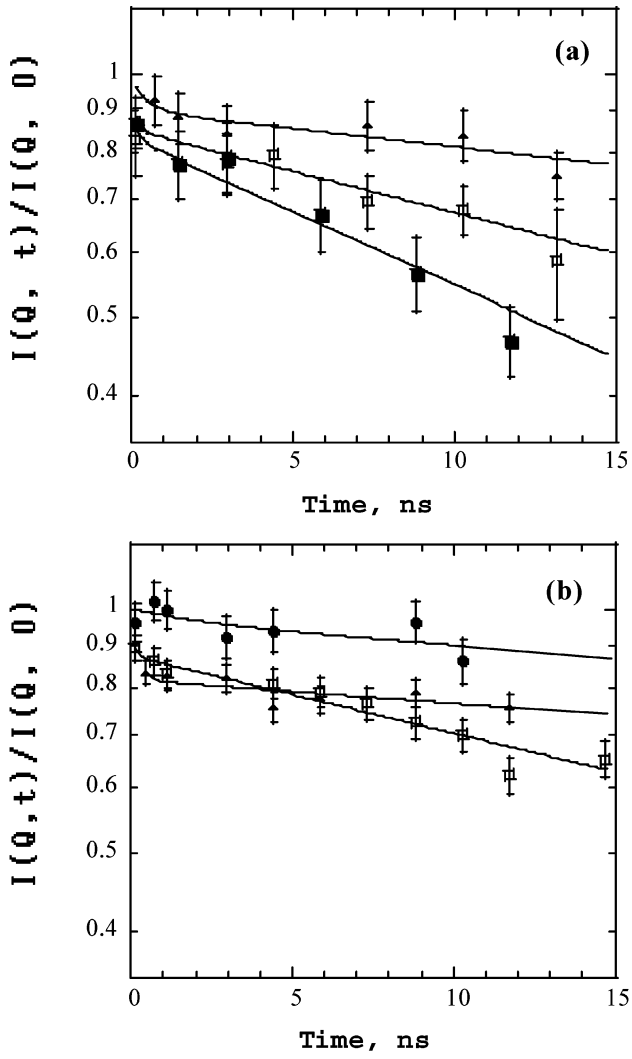

Figure 7. Normalized intermediate scattering function $I(Q,t)/I(Q,0)$, as a function of time t, for 1.0 wt % solutions of G5 dendrimers. (a) OH−PAMAM dendrimer and (b) sugar ball. Solid lines are theoretical ones calculated with a double-decaying exponential function (eqs 6−8). Legend of symbols is the same as the legends in Figures 3 and 4.

Kanaya et al.[40] applied the breathing mode motion, which was theoretically predicted by de Gennes,[41] to explain NSE results for polymer micelles. Our results are not explainable by this mode. Matsuoka et al.[9] investigated the dynamic behavior of micelles of amphiphilic diblock copolymers in aqueous solutions by NSE. Using the double-exponential function like in our analysis, the slow and fast modes were assigned to the translational diffusion and the internal motion, respectively, of the polymer micelle.

In our case, two dendrimers with different types of end groups in aqueous solutions showed the same behavior regarding to the dynamics of the fast mode. In other words, the fast mode, which was not expected from the theoretical analysis carried out by Ganazzoli et al.,[29] is independent of the end groups of the dendrimer. Then, this novel dynamics, which is faster than

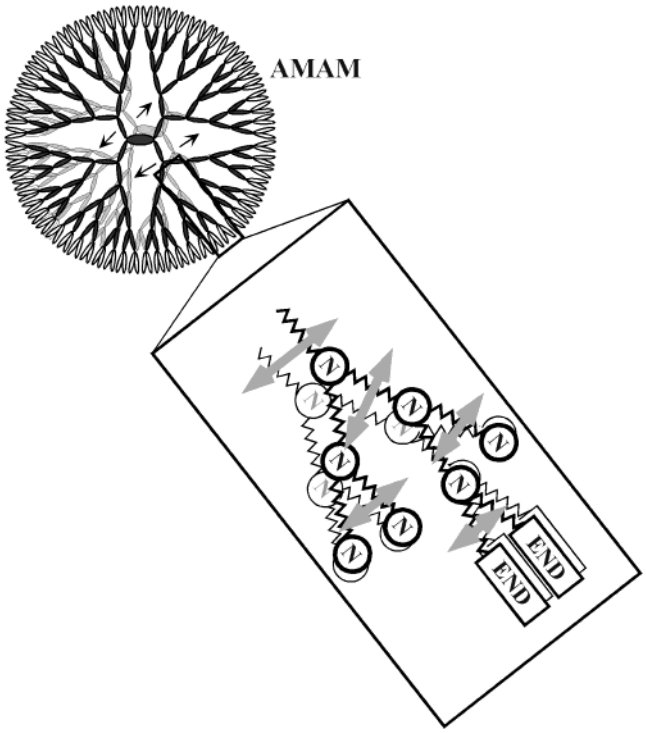

Figure 8. Schematic representation of segmental motions in G5 dendrimers with internal segments of amido-amine repeating units.

the translational diffusion of the dendrimers, must be characteristics of amido-amine segments, which are common in both dendrimers, as illustrated in Figure 8. Although the fast diffusion mode is expected to be caused by the segment motion in the dendrimers, this novel microscopic dynamics of dendrimers has very complex properties, relating to the chemical structures of segments, interior or exterior voids, the branching architectures, and so on.

Conclusions

The dynamics of G5 PAMAM dendrimers with different types of end groups in D_2O solutions were investigated by NSE experiments. The behaviors were same for both, OH−PAMAM dendrimers and sugar balls, but different at 0.1 and 10 wt % concentrations.

For the solutions at a high concentration, the intermediate correlation functions obeyed a single-decaying equation. The effective diffusion coefficient D_{eff} showed a remarkable Q dependence, which is attributed to the dendrimer−dendrimer interactions, since it is consistent with the Q dependence of $S(Q)$ evaluated by SANS.

On the contrary, two relaxation modes were observed at a low concentration, where the inter-dendrimer structure factor $S(Q)$ can be ignored. The slow mode corresponds to the translational diffusion of the dendrimer. The fast mode is attributed to the segment motion in the dendrimers, though its contribution is small. It seems that the amido-amine segments originate this fast mode, being common to both dendrimers.

The dynamics of the dendrimers does not depend on the type of end groups used in the present work. However, the different dynamical behaviors depending on the dendrimer concentration are important to discuss the doping function of dendrimers in solution. The effect observed here for the segmental motion in globular dendrimers on the intermediate scattering function $I(Q,t)/I(Q,0)$, obtained from NSE, must be further confirmed even in other systems according to the adequate analysis. Therefore, we expect the results obtained here will promote future experimental developments and theoretical analysis of the dynamics of different molecules with well-defined architectures.

Acknowledgment. The authors are grateful to Drs. T. Otomo, S. Shimizu, and T. Adachi at KEK for their help on the SANS measurements. The experiments at JRR-3 were done under the approval of the Neutron Scattering Program Advisory Committee (Proposals 99-050 and 99-194).

References and Notes

(1) Mezei, F., Ed. *Neutron Spin−Echo Proceedings, Lecture Notes in Physics*; Springer: Berlin, 1979; p 128.

(2) Kanaya, T.; Kaji, K.; Kitamaru, R.; Higgins, J. S.; Farago, B. *Macromolecules* **1989**, *22*, 1356.

(3) Farago, B.; Monkenbrusch, M.; Richter, D.; Huang, J. S.; Fetters, L. J.; Gast, A. P. *Phys. Rev. Lett.* **1993**, *71*, 1015.

(4) Ewen, B.; Richter, D. *Macromol. Symp.* **1995**, *90*, 131.

(5) Richter, D. *Hyperfine Interact.* **1997**, *106*, 3.

(6) Arbe, A.; Buchenau, U.; Willner, L.; Richter, D.; Farago, B.; Colmenero, *J. Phys. Rev. Lett.* **1996**, *76*, 1872.

(7) Richter, D.; Arbe, A.; Colmenero, J.; Monkenbusch, M.; Farago, B.; Faust, R. *Macromolecules* **1998**, *31*, 1133.

(8) Monkenbusch, M.; Goecking, K. D.; Schneiders, D.; Richter, D.; Fetters, L. J.; Huang, J. S. *Prog. Colloid Polym. Sci.* **1997**, *106*, 1112.

(9) Matsuoka, H.; Yamamoto, Y.; Nakano, M.; Endo, H.; Yamaoka, H.; Zorn, R.; Monkenbusch, M.; Richter, D.; Seto, H.; Kawabata, Y.; Nagao, M. *Langmuir* **2000**, *16*, 9177.

(10) Monkenbusch, M.; Schätzler, R.; Richter, D. *Nucl. Instrum. Methods Phys. Res.* **1997**, A *399*, 301.

(11) Arbe, A.; Monkenbusch, M.; Stellbrink, J.; Richter, D.; Farago, B.; Almdal, K.; Faust, R. *Macromolecules*, **2001**, *34*, 1281.

(12) (a)Tomalia, D. A.; Baker, H.; Dewald, J.; Hall, M.; Kallos, G.; Martin, S.; Roeck, J.; Ryder, J.; Smith, P. *Polym. J.* **1985**, *17*, 117. (b)-Tomalia, D. A.; Naylor, A. M.; Goddard, W. A. III *Angew. Chem., Int. Ed. Engl.* **1990**, *29*, 138.

(13) (a) Frechét, J. M. J. *Science* **1994**, *263*, 1710. (b) Frechét, J. M. J.; Henmi, M.; Gitsov, I.; Aoshima, S.; Leduc, M. R.; Grubbs, R. B. *Science* **1995**, *269*, 1080.

(14) Bauer, B. J.; Briber, R. M.; Hammouda, B.; Tomalia, D. A. *Polym. Mater. Sci. Eng.* **1992**, *66*, 428.

(15) Briber, R. M.; Bauer, B. J.; Hammouda, B.; Tomalia, D. A. *Polym. Mater. Sci. Eng.* **1992**, *66*, 430.

(16) Scherrenberg, R.; Coussens, B.; van Vliet, P.; Edouard, G.; Brackman, J.; de Brabander, E.; Mortensen, K. *Macromolecules* **1998**, *31*, 456.

(17) Ramzi, A.; Scherrenberg, R.; Brackman, J.; Joosten, J.; Mortensen, K. *Macromolecules* **1998**, *31*, 1621.

(18) Imae, T.; Funayama, K.; Aoi, K.; Tsutsumiuchi, K.; Okada, M.; Furusaka, M. *Langmuir* **1999**, *15*, 4076.

(19) Funayama, K.; Imae, T. *J. Phys. Chem. Solids* **1999**, *60*, 1355.

(20) Pötschke, D.; Ballauff, M.; Lindner, P.; Fischer, M.; Vögtle, F. *Macromolecules* **1999**, *32*, 4079.

(21) Ramzi, A.; Bauer, B. J.; Scherrenberg, R.; Froehling, P.; Joosten, J.; Amis, E. J. *Macromolecules* **1999**, *32*, 4983.

(22) Nisato, G.; Ivkov, R.; Amis, E. J. *Macromolecules* **1999**, *32*, 5895.

(23) Topp, A.; Bauer, B. J.; Klimash, J. W.; Spindler, R.; Tomalia, D. A.; Amis, E. J. *Macromolecules* **1999**, *32*, 7226

(24) Funayama, K.; Imae, T.; Aoi, K.; Tsutsumiuchi, K.; Okada, M.; Seto, H.; Nagao, M. *J. Phys. Soc. Jpn* **2001**, *70*, Suppl. A, 326.

(25) Aoi, K.; Tsutsumiuchi, K.; Yamamoto, A.; Okada, M. *Macromol. Rapid Commun.* **1998**, *19*, 5.

(26) Tsutsumiuch, K.; Aoi, K.; Okada, M. *Polym. J.* **1999**, *31*, 935.

(27) Stark, B.; Stühn, B.; Frey, H.; Lach, C.; Lorenz, K.; Frick, B. *Macromolecules* **1998**, *31*, 5415.

(28) Chen, Z. Y.; Cai, C. *Macromolecules* **1999**, *32*, 5423.

(29) Ganazzoli, F.; Ferla, R. L.; Raffaini, G. *Macromolecules* **2001**, *34*, 4222.

(30) Glatter, O.; Kracky, O. *Small-Angle X-ray Scattering*; Academic Press: London, 1982.

(31) Chen, S. H. *Annu. Rev. Phys. Chem.* **1986**, *37*, 351.

(32) Chen, S. H.; Lin, T. L. *Method Exp. Phys.* **1987**, *23*, 489.

(33) Takeda, T.; Komura S.; Seto, H.; Nagao, M.; Kobayashi, H.; Yokoi, E.; Ebisawa, T.; Tasaki, S.; Zeyen, C. M. E.; Ito, Y.; Takahashi, S.; Yoshizawa, H. *Phys. B* **1995**, *213&214*, 863.

(34) Takeda, T.; Seto, H.; Kawabata, D.; Krist, T.; Zeyen, C. M. E.; Anderson, I. S.; Høghøj, P.; Nagao, M.; Yoshizawa, H.; Komura S.; Ebisawa, T.; Tasaki, S.; Monkenbusch, M. *J. Phys. Chem. Solids* **1999**, *60*, 1599.

(35) Funayama, K.; Imae, T.; Aoi, K.; Tsutsumiuchi, K.; Okada, M.; Furusaka, M. Nagao, M. *J. Phys. Chem. B*, in press.

(36) Hayter, J. B.; Jannink, G.; Nallet, F.; Brochard-Wyart, F.; de Gennes, P. G. *J. Phys. Lett.* **1980**, *41*, L-451.

(37) Huang, J. S.; Milner, S. T.; Farago, B.; Richter, D. *Phys. Rev. Lett.* **1987**, *59*, 2600.

(38) Farago, B.; Richter, D.; Huang, J. S.; Safran, S. T.; Milner, S. T. *Phys. Rev. Lett.* **1990**, *65*, 3348.

(39) Komura, S.; Seto, H.; Takeda, T. *Prog. Colloid Polym. Sci.* **1997**, *106*, 11.

(40) Kanaya, T.; Monkenbusch, M.; Richter, D. Unpublished data.

(41) de Gennes, P. G. *C. R. Acad. Sci. Paris Ser. II* **1986**, *302*, 765.